Monitoring the Conformational Fluctuations of DNA Hairpins Using Single-Pair Fluorescence Resonance Energy Transfer

Jocelyn R. Grunwell,*,† Jennifer L. Glass,‡,§ Thilo D. Lacoste,§ Ashok A. Deniz,†,⊥ Daniel S. Chemla,‡,§ and Peter G. Schultz‡,⊥

Contribution from the Departments of Chemistry and Physics, University of California, Berkeley, California 94720, and Materials Sciences Division, Lawrence Berkeley National Laboratory, Berkeley, California 94720

Received July 26, 2000. Revised Manuscript Received February 28, 2001

Abstract: We present single-pair fluorescence resonance energy transfer (spFRET) observations of individual opening and closing events of surface-immobilized DNA hairpins. Two glass−surface immobilization strategies employing the biotin−streptavidin interaction and a third covalent immobilization strategy involving formation of a disulfide bond to a thiol-derivatized glass surface are described and evaluated. Results from image and time-trace data from surface-immobilized molecules are compared with those from freely diffusing molecules, which are unperturbed by surface interactions. Using a simple two-state model to analyze the open and closed time distributions for immobilized hairpins, we calculate the lifetimes of the two states. For hairpins with a loop size of 40 adenosines and a stem size of either seven or nine bases, the respective closed-state lifetimes are 45 ± 2.4 and 103 ± 6.0 ms, while the respective open-state lifetimes are 133 ± 5.5 and 142 ± 22 ms. These results show that the open state of the hairpin is favored over the closed state of the hairpin under these conditions, consistent with previous diffusion fluorescence correlation spectroscopy (FCS) experiments on poly(A)-loop hairpins. The measured open-state lifetime is about 30 times longer than the calculated 3 ms open-state lifetime for both hairpins based on a closing rate scaling factor derived from a previous FCS study for hairpins in diffusion with 12−30 thymidines in their loops. As predicted, the closed-state lifetime is dependent on the stem length and is independent of the loop characteristics. Our findings indicate that current models should consider sequence dependence in calculating ssDNA thermostability. The surface immobilization chemistries and other experimental techniques described here should prove useful for studies of single-molecule populations and dynamics.

Introduction

DNA hairpins are inverse repeats of single-stranded DNA connected by a noncomplementary loop sequence, and they are one of the simplest structures that a nucleic acid polymer can form. Hairpins are often found at replication origins, promoters, operator sequences, and other sites of regulation in genomic DNA and are thus thought to play a critical role in the regulation of gene transcription, DNA recombination, and DNA replication.[1−4] For example, multiple alternative forms of hairpin structures can result in a variety of genetic disorders,[5,6] and hairpin structures mediate the interacting hairpin loops, or "kissing complexes", of HIV dimerization.[7,8] DNA hairpins are proposed anti-sense drugs due to their high resistance to nuclease degradation, and DNA hairpin molecular beacons, in conjunction with gene chip technology, are useful tools in disease diagnostics and drug development.[9−14] Because DNA hairpins are known to show two-state folding kinetics, they can serve as a model system for the study of single-molecule kinetics on surfaces.

DNA hairpins fluctuate in solution between a folded (closed) state and a denatured (open) state. This two-state transition is an equilibrium process that can be described by the following equations and as illustrated in Figure 1.

$$K_{\text{closed}} = \frac{k_{\text{closed}}[\text{open hairpin}]}{k_{\text{open}}[\text{closed hairpin}]} \quad (1)$$

$$\Delta G_{\text{closed}} = -RT \ln(K_{\text{closed}}) \quad (2)$$

The closed state is characterized by lower enthalpy than the

* To whom correspondence should be addressed.
† Department of Chemistry, University of California, Berkeley.
‡ Department of Physics, University of California, Berkeley.
§ Lawrence Berkeley National Laboratory.
⊥ Present address: The Skaggs Institute of Chemical Biology, The Scripps Research Institute, La Jolla, CA 92037.

(1) Mariappan, S. V. S.; Catasta, P.; Chen, X.; Ratliff, R.; Moyzis, R. K.; Bradbury, E. M.; Gupta, G. *Nucleic Acids Res.* **1996**, *24*, 784−792.
(2) Rosenberg, M.; Court, D. *Annu. Rev. Genet.* **1979**, *13*, 319−353.
(3) Amir-Aslani, A.; Mauffret, O.; Bittoun, P.; Sourgen, F.; Monnot, M.; Lescot, E.; Fermandijan, S. *Nucleic Acids Res.* **1995**, *23*, 3850−3857.
(4) Chen, X.; Mariappan, S. V.; Catasti, P.; Ratliff, R.; Moyzis, R. K.; Laayoun, A.; Smith, S. S.; Bradbury, E. M.; Gupta, G. *Proc. Natl. Acad. Sci. U.S.A.* **1995**, *92*, 5199−5203.
(5) Mariappan, S. V. S.; Garcie, A. E.; Gupta, G. *Nucleic Acids Res.* **1996**, *24*, 775−783.
(6) Skripkin, E.; Paillart, J. C.; Marquet, R.; Ehresmann, B.; Ehresmann, C. *Proc. Natl. Acad. Sci. U.S.A.* **1994**, *91*, 4945−4949.
(7) Tyagi, S.; Kramer, F. R. *Nat. Biotechnol.* **1996**, *14*, 303−308.
(8) Muriaux, D.; Fosse, P.; Paoletti, J. *Biochemistry* **1996**, *35*, 5075−5082.
(9) Tyagi, S.; Bratu, D. P.; Kramer, F. R. *Nat. Biotechnol.* **1998**, *16*, 49−53.
(10) Kostrikis, L. G.; Huang, Y. X.; Moore, J. P.; Wolinsky, S. M.; Zhang, L. Q.; Guo, Y.; Deutsch, L.; Phair, J.; Neumann, A. U.; Ho, D. D. *Nat. Med.* **1998**, *4*, 350−353.
(11) Kostrikis, L. G.; Tyagi, S.; Mhlanga, M. M.; Ho, D. D.; Kramer, F. R. *Science* **1998**, *279*, 1228−1229.
(12) Piatek, A. S.; Tyagi, S.; Pol, A. C.; Telenti, A.; Miller, L. P.; Kramer, F. R.; Alland, D. *Nat. Biotechnol.* **1998**, *16*, 359−363.

10.1021/ja0027620 CCC: $20.00
Published on Web 04/17/2001

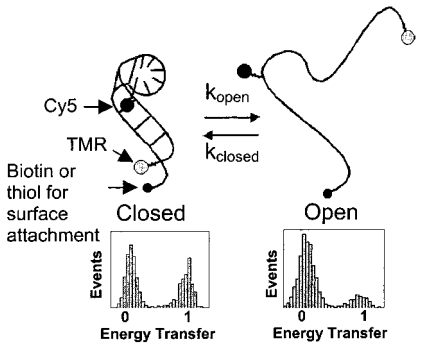

Figure 1. Schematic of the closed-to-open transition of a DNA hairpin with the approximate position of the donor and acceptor fluorophores for the hairpins used in the kinetics measurements. The third smaller ball at the 3′ end of the hairpin indicates the biotin or thiol functionality used for surface attachment. The expected energy transfer efficiency for the folded state is indicated by the simulated spectrum below the native hairpin. The histogram underneath the closed hairpin has a larger peak at a FRET efficiency near 1 than the open hairpin. A denatured hairpin is a single strand of DNA that acts as a random coil. Very little energy transfer will occur, as shown by the increase in the peak at zero in the histogram below the open hairpin. There is a peak at zero energy transfer efficiency underneath the closed hairpin due to photobleaching of the acceptor fluorophore, which causes an immediate rise in donor dye fluorescence and a halt to energy transfer.

open state due to base pairing and stacking. The open state is characterized by high entropy, as a large number of configurations are possible from a single strand of DNA. Many thermodynamic and structural studies have been performed on DNA hairpins to understand the energetics of nucleic acid folding and to derive accurate parameters for predicting the stability of various sequences involved in forming DNA secondary structure.[15,16]

There are very few studies on the kinetics of hairpin folding.[17,18] The opening rate depends on the unzipping energy of the hairpin, while the closing rate relies on the collision of the two stalks of the stem, followed by nucleation and the propagation of base-pairing. Recent work used fluorescence correlation spectroscopy (FCS) and fluorescence quenching, with an average of five hairpins in the excitation beam, to show that the rate of opening of the hairpin stem was essentially independent of the loop characteristics regardless of loop size, sequence, and NaCl concentration.[19] The rate of hairpin closing scaled with the loop length and rigidity; an adenosine loop led to smaller closing rates and higher activation energies than a thymidine loop of the same size.

Single-molecule experiments can reveal the subpopulations and dynamics of an inhomogeneous biochemical system that are otherwise hidden in ensemble measurements. The number and scope of single-molecule fluorescence experiments are increasing dramatically, and single-molecule detection and spectroscopy are finding practical applications in the study of many interesting biological systems including protein folding, enzymatic dynamics studies, and ligand−receptor interactions.[20−25] Fluctuations of individual biological constructs may be monitored in real time and statistically analyzed to reveal distributions in rates of folding or in enzymatic turnover.[26] To monitor folding processes, it is often desirable to isolate a single molecule and to watch its behavior over time. Since single-molecule diffusion measurements of molecules that exhibit fluctuations slower than the rate of the diffusion transit time through the excitation region will show only the equilibrium population distribution of the molecules rather than the actual fluctuation events, these molecules must be immobilized in a gel or on a surface. Single-molecule experiments may allow us to understand the complex kinetic behavior of hairpin formation at regulation sites in the genome. Ratiometric FRET measurements coupled with gene chip technology may allow for rapid genetic screening and should prove to be a useful diagnostic tool.

For single-molecule experiments, we designed hairpins to open and close on a time scale of 0.2 ms or greater. Extrapolating from the data reported by Bonnet et al. using a scaling factor of 3, we predicted an open-state lifetime of about 3 ms for our hairpins with a stem length of either seven or nine base pairs and a loop of 40 adenosines.[19] Using $\Delta G°$ calculations based on a nearest-neighbor prediction of DNA oligomer stability by SantaLucia and using the open-state lifetime predicted from the work of Bonnet et al. mentioned above, we predicted a closed-state lifetime of approximately 70 ms and 3.8 s for the seven-base-pair stemmed and the nine-base-pair stemmed hairpins, respectively.[27,28] The predicted closed-state lifetimes may not be accurate, however, as the nearest-neighbor theory predicts closed-state lifetimes to be 30 times longer than the measured lifetime for a hairpin with five base pairs in the stem and 21 adenosines in the loop from the study reported by Bonnet et al., and the calculated $\Delta G°$ to be more stable than the experimental value by an order of magnitude. Interestingly, the nearest-neighbor theory predicts the $\Delta G°$ of hairpins with the same five-base-pair stem with 12, 16, 21, or 30 thymidines in their loops to within a 20% error from the same FCS study.[19] We demonstrate three different surface immobilization strategies. Streptavidin was either reacted with an epoxide-derivatized glass surface[29,30] or immobilized through a non-specifically adsorbed biotinylated bovine serum albumin (BSA)-coated glass surface in order to exploit streptavidin's strong interaction with biotin.[31] Finally, we modified a method for single-molecule studies that cross-links hairpins to glass through a disulfide

(13) Fang, X.; Liu, X.; Schuster, S.; Tan, W. *J. Am. Chem. Soc.* **1999**, *121*, 2921−2922.
(14) Erie, D. A.; Suri, A. K.; Breslauer, K. J.; Jones, R. A.; Olson, W. K. *Biochemistry* **1993**, *32*, 436−454.
(15) Antao, V., P.; Lai, S. Y.; Tinoco, I., Jr. *Nucleic Acids Res.* **1991**, *19*, 5901−5905.
(16) Varani, G. *Annu. Rev. Biophys. Biomol. Struct.* **1995**, *24*, 379−404.
(17) Gralla, J.; Crothers, D. M. *J. Mol. Biol.* **1971**, *73*, 497−511.
(18) Hilbers, C. W.; Haasnoot, C. A.; de Bruin, S. H.; Jorden, J. J.; van der Marel, G. A.; van Boom, J. H. *Biochimie* **1985**, *67*, 685−695.
(19) Bonnet, G.; Krichevsky, O.; Libchaber, A. *Proc. Natl. Acad. Sci. U.S.A.* **1998**, *95*, 8602−8606.
(20) Schutz, G. J.; Trabesinger, W.; Schmidt, T. *Biophys. J.* **1998**, *74*, 2223−2226.
(21) Lu, H. P.; Xun, L. Y.; Xie, X. S. *Science* **1998**, *282*, 1877−1882.
(22) Ishii, Y.; Yoshida, T.; Funatsu, T.; Wazawa, T.; Yanagida, T. *Chem. Phys.* **1999**, *247*, 163−173.
(23) Deniz, A. A.; Laurence, T. A.; Beligere, G. S.; Dahan, M.; Martin, A. B.; Chemla, D. S.; Dawson, P. E.; Schultz, P. G.; Weiss, S. *Proc. Natl. Acad. Sci. U.S.A.* **2000**, *97*, 5179−5184.
(24) Ha, T.; Ting, A. Y.; Liang, J.; Caldwell, W. B.; Deniz, A. A.; Chemla, D. S.; Schultz, P. G.; Weiss, S. *Proc. Natl. Acad. Sci. U.S.A.* **1999**, *96*, 893−898.
(25) Noji, H.; Yasuda, R.; Yoshida, M.; Kinosita, K. *Nature* **1997**, *386*, 299−302.
(26) Schroth, G. P.; Ho, P. S. *Nucleic Acids Res.* **1995**, *23*, 1977−1983.
(27) SantaLucia, J. J. *Proc. Natl. Acad. Sci. U.S.A.* **1998**, *95*, 1460−1465. $\Delta G°$ calculations were performed at the following website: http://bioinfo.math.rpi.edu/~mfold/dna/form1.cgi.
(28) SantaLucia, J. J.; Zuker, M.; Bommarito, A.; Irani, R. J., unpublished results, 1999.
(29) Wennmalm, S.; Edman, L.; Rigler, R. *Proc. Natl. Acad. Sci. U.S.A.* **1997**, *94*, 10461−10466.
(30) Edman, L.; Földes-Papp, Z.; Wennmalm, S.; Rigler, R. *Chem. Phys.* **1999**, *247*, 11−22.
(31) Ha, T.; Zhuang, X.; Kim, H. D.; Orr, J. W.; Williamson, J. R.; Chu, S. *Proc. Natl. Acad. Sci. U.S.A.* **1999**, *96*, 9077−9082.

bond.[32] We monitored diffusing hairpin folding as a function of temperature, and we observed exponential kinetics for the opening and closing of hairpins immobilized on a surface.

spFRET

Fluorescence resonance energy transfer is a powerful spectroscopic technique that allows biologically relevant distances between 20 and 80 Å to be quantified under physiological conditions with near-angstrom resolution due to the strong distance dependence of the transfer process. FRET is the nonradiative transfer of energy from a donor molecule to an acceptor molecule that occurs through a dipole−dipole interaction.[33] When two fluorescent molecules are used, FRET results in a decrease in donor fluorophore emission intensity with a simultaneous increase in acceptor fluorophore emission intensity. FRET depends on the inverse sixth power of the distance between the two fluorophores (R^{-6}), which allows spFRET to act as a sensitive molecular ruler in biological systems.[34,35] Distance and orientation information on biomolecules is obtained when changes in energy transfer and fluorescence anisotropy of the dyes are quantified.

There are several expressions for the efficiency, E, of energy transfer.[36,37] Because our experiments involve the measurements of the intensities of the donor and acceptor fluorescence, we employ an expression of the form

$$E = \frac{{R_o}^6}{{R_o}^6 + R^6} = \frac{I_A}{I_A + \gamma I_D} \qquad (3)$$

in which I_A and I_D are the measured intensities of the acceptor and donor fluorophores, respectively, R is the distance between the two fluorophores, R_o is the Förster radius, or distance of 50% energy transfer, and γ is an experimental factor that includes the ratios of the donor and acceptor fluorophore quantum efficiencies as well as the efficiencies of detection for the two fluorophores. For the donor fluorophore, tetramethylrhodamine (TMR), and the acceptor fluorophore, Cy5, dye pair, the value of γ is estimated to be 0.8 for our measurements.[24] The value of R_o depends on several factors, including an orientational factor, κ^2, described later, and the spectral overlap of the donor emission and the acceptor absorption. The normalized TMR emission spectrum, the Cy5 absorption and emission spectra, and the structures of both TMR and Cy5 are shown in Figure 2. The spectra in Figure 2 also show that excitation of TMR at 514 nm causes very little direct excitation of Cy5, and that leakage of the TMR fluorescence onto the Cy5 fluorescence detector accounts for less than 15% of the Cy5 signal.

Materials and Methods

All DNA synthesis reagents including amino modifier C6 dT (dTC_6-NH_2), 5′-thiol-modifier C6, and 1 μM biotin triethyleneglycol controlpore glass resin (Btn TEG CPG) phosphoramidites were purchased from Glen Research. The maleimide derivative of tetramethylrhodamine (TMR-maleimide) was purchased from Molecular Probes, and the *N*-hydroxysuccinimidyl ester of cyanine 5 (Cy5-NHS) was purchased from Amersham. Enzymes were purchased from New England Biolabs.

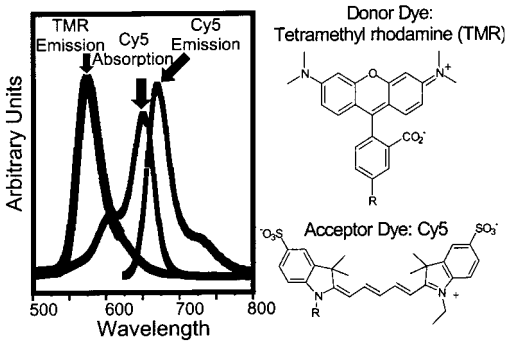

Figure 2. Spectral overlap between TMR emission and Cy5 absorption, shown on a graph of wavelength versus arbitrary units. Excitation of the donor dye, TMR, occurs at 514 nm, and direct excitation and leakage of the TMR signal onto the acceptor fluorophore, Cy5, detector account for less than 15% of the acceptor fluorophore signal. The R groups of the dyes are linkers with a maleimide, an *N*-hydroxysuccinimidyl ester, or a phosphoramidite group, depending on the labeling strategy used in the oligonucleotide synthesis, as described in the Materials and Methods section.

Sequences of the Hairpins Studied. dA40s7 HP Btn: 5′-TMR-SC_6-CTCTTCA-$(AAA)_{13}$A-dTC_6NH-(Cy5)-GAAGAG-TEGBtn-3′. dA40s9 HP Btn: 5′-TMR-SC_6-CTCTTCAGT-$(AAA)_{13}$A-$ACdTC_6$NH-(Cy5)-GAAGAG-TEGBtn-3′. dA40s9 HP Thiol: 5′-Cy5-CTCTTCAGT-$(AAA)_{13}$A-$ACdTC_6$NH-(TMR)-GAAGAG-TEG_{18} C_6S-SdT-3′. dA30s14 HP Thiol: 5′-Cy5-CTCTTCAGTTCACA-$(AAA)_{10}$-TGTGAA$CdTC_6$-NH-(TMR)-GAAGAG-TEG_{18} C_6S-SdT-3′.

Hairpin labeling uses the following scheme. The "d" is used to indicate that deoxyribonucleotides are used to synthesize the hairpins. The "A30" and "A40" are used to indicate that there are either 30 or 40 adenosines in the loop of the hairpin. The "s" followed by a number refers to the number of base pairs in the stem of the hairpin.

Sample Preparation. (a) DNA Synthesis: dA40S7 HP Btn and dA40S9 HP Btn. Synthesis of these hairpins was accomplished using standard β-cyanoethyl phosphoramidite chemistry on a DNA synthesizer (Applied Biosystems). The hairpin was deprotected with 1 mL of concentrated NH_4OH for 12 h at 55 °C and concentrated by centrifugation under vacuum. The oligonucleotide was purified on a C_{18} reversed-phase semipreparative protein−peptide column using a gradient of 5% to 45% CH_3CN in 0.05 M tetraethylammonium acetate (TEAA), pH 7, over a 30 min period. All hairpin species were analyzed by electrophoresis on a 15% denaturing polyacrylamide gel and imaged visually if dye labeled and by standard ethidium bromide staining. All hairpins were shown to have approximately a 1:1:1 absorbance ratio for DNA:TMR:Cy5 at their respective absorbance maxima.

(b) TMR-Maleimide Labeling and Cy5-NHS Ester Labeling. The oligonucleotides were labeled according to the procedures previously described.[35]

(c) dA40S9-3′ Biotin-Modified Hairpin. It was difficult to obtain significant quantities of full-length hairpin by total synthesis due to the size of the hairpin and the many adenosine−adenosine couplings in the synthesis for both the dA40S7 and the dA40S9 hairpins. An alternative strategy was utilized for synthesizing additional dA40S9 Btn hairpin by ligating together two dye-labeled oligonucleotide fragments of the hairpin together with a complementary oligonucleotide splint and T4 DNA ligase. The oligonucleotide fragments were synthesized and purified as described above. The 5′ fragment of the hairpin incorporated a trityl-protected 5′-thiol modifier C6, while the 3′ fragment incorporated an amino modifier C6 dT and either a 1 μM biotin TEG CPG phosphoramidite or a 3′ thiol-modified CPG phosphoramidite. The 5′ end of the biotinylated fragment was phosphorylated using T4 polynucleotide kinase (PNK).

(d) Phosphorylation of the 5′ End of the Biotinylated DNA Hairpin Fragment. To a 215 nM concentration of biotinylated DNA

(32) Rogers, Y.-H.; Jiang-Baucom, P.; Huang, Z.-J.; Bogdanov, V.; Anderson, S.; Boyce-Jacino, M. T. *Anal. Biochem.* **1999**, *26*, 23−30.
(33) Förster, T. *Modern Quantum Chemistry*; Academic Press: New York, 1966.
(34) Stryer, L.; Haugland, R. P. *Proc. Natl. Acad. Sci. U.S.A.* **1967**, *58*, 719−730.
(35) Deniz, A.; Dahan, M.; Grunwell, J. R.; Ha, T.; Faulhaber, A. E.; Chemla, D. S.; Weiss, S.; Schultz, P. G. *Proc. Natl. Acad. Sci. U.S.A.* **1999**, *96*, 3670−3675.
(36) Cantor, C. R.; Schimmel, P. R. *Biophysical Chemistry*; Freeman: San Francisco, 1980.
(37) Meer, B. *Resonance Energy Transfer: Theory & Data*; VCH: New York, 1994.

in 480 μL of sterile double-distilled water (ddH_2O) was added 60 μL of 10× T4 DNA ligase buffer, 50 μL of ddH_2O, and 100 units of T4 PNK. The reaction tube was briefly centrifuged and incubated at 37 °C for 3 h. The kinase reaction was purified by phenol:chloroform extraction, and the DNA was ethanol precipitated. The thiol-containing oligonucleotide was labeled with TMR-maleimide, while the phosphorylated, biotinylated, and amine-containing oligonucleotide was labeled with Cy5-NHS ester. Free dye was removed by running a NAP 5 column followed by size-exclusion FPLC on a Superdex 75 column (Pharmacia). The labeled hairpin fragments were then HPLC purified as described above to separate unlabeled DNA from labeled DNA.

(e) Ligation of the Dye-Labeled DNA Hairpin Fragments. A 3.5 nM concentration of the TMR-labeled oligonucleotide, a 4.3 nM concentration of the Cy5-labeled oligonucelotide, and a 4.5 nM concentration of the splint oligonucleotide were mixed in a centrifuge tube. The mixture was concentrated to dryness by vacuum centrifugation, followed by resuspension in 16 μL of ddH_2O. To the resuspended mixture were added 2 μL of 10× T4 DNA ligase buffer and 10 units of T4 DNA ligase. The ligation reaction was run at 16 °C overnight. The ligated hairpin was purified by size exclusion FPLC on a Superdex 75 column to separate the hairpin from the individual dye-labeled oligonucleotides and the splint oligonucleotide. The ligated product was analyzed by using a 15% denaturing polyacrylamide gel.

(d) dA40S9 HP Thiol and dA30S14 HP Thiol. These hairpins were purchased from Synthegen. Cy5 was incorporated into the DNA as the final phosphoramidite in the synthesis. Large control-pore glass resin was used to accommodate the length and multiple adenosine-to-adenosine couplings. The 3′ thiol was protected by a disulfide bond to a thiol-modified thymidine. An 18-TEG phosphoramidite was used as a spacer between the DNA hairpin and the 3′ thiol surface attachment.

Surface Preparations. (a) Biotin−Streptavidin Immobilization of DNA Hairpins to Glass Cover Slips. Gold Seal Clay Adams cover slips (No. 1, VWR Scientific) were cut in half and soaked in 5% HF acid for 2 min. The cover slips were washed twice with ddH_2O and were again soaked in 5% HF for 2 min. The cover slips were washed twice with ddH_2O, dried with N_2, and silanized by adding 10 μL of distilled 3-glycidoxypropyltrimethoxysilane (Aldrich) to the center of the cover slip and incubating in a HF-cleaned glass Petri dish for 5 min. The silanized cover slip was washed with ddH_2O, dried with N_2, and reacted with 10 μL of a 0.1 mg/mL solution of streptavidin in 10 mM Na_2CO_3 buffer, pH 9, for 5 min. The cover slip was washed with ddH_2O and dried with N_2. The remaining epoxides were quenched with 10 μL of 2 mM aspartic acid in a 0.5 M carbonate buffer, pH 9, followed by a ddH_2O washing/N_2 drying step. Attachment of the hairpin to the cover slip was accomplished by reacting 10 μL of a 200 nM biotinylated DNA hairpin in a 50 mM PBS buffer, pH 7.0, with the cover slip for 5−15 min, followed by a final ddH_2O washing/N_2 drying step.

(b) Biotinylated BSA and Streptavidin Surfaces. VWR Brand No. 1 glass cover slips were cleaned by a 20 min sonication followed by soaking in 1 M KOH in a staining dish for a minimum of 3 h. Cover slips were then rinsed in ddH_2O and dried with N_2. Following the method of Gaub and co-workers,[38] 50 μL of a 29 μM solution of biotinylated BSA (Pierce) was placed on the cover slip and incubated for 10 min. The cover slip was washed with ddH_2O and dried with N_2, and then 10 μL of a 0.1 mg/mL solution of streptavidin (Pierce) was incubated on the surface for 10 min. After incubation, the cover slip was once again washed and dried, and a 10 μL drop of 50 nM biotinylated DNA was incubated on the surface for 30 min, followed by a final ddH_2O washing/N_2 drying step.

(c) Disulfide Bond Immobilization of DNA Hairpins to Glass Cover Slips. The following procedure was adapted from Rogers et al.[32] VWR Brand No. 1 glass cover slips were cleaned by first sonicating for 30 min and then soaking in a 1 M KOH solution in a staining dish for a minimum of 3 h. Cover slips were rinsed in bulk three times with a staining dish volume full of ddH_2O. The slips were then incubated in a 1% 3-mercaptopropyl triethoxysilane (MPTS) (Fluka) solution in a 0.1 M NaH_2PO_4 solution at pH 6 for 45 min to 1 h. The MPTS solution was shaken periodically to disperse the silane, which forms an emulsion in the phosphate buffer. The cover slips were then rinsed in bulk once with 0.1 M NaH_2PO_4, pH 6, followed by a single bulk rinse with ddH_2O. The slips were individually rinsed with ddH_2O and dried with a stream of N_2. The slips were placed in the covered staining dish and were cured for 30 min in a glassware-drying oven at 175 °C. After curing, the cover slips were rinsed individually with a 0.05% solution of Tween 20, followed by a ddH_2O washing/N_2 drying step. A 100 pM solution of DNA hairpin in a 0.5 M $NaHCO_3$, pH 9 buffer, was incubated on the surface for 10 min. The sample was rinsed with ddH_2O and dried with N_2. For all surface preparations, the slips were stored in a N_2 glovebox until use. Cover slips more than 10 h old were discarded, and blank cover slips were examined to ensure that there were no false fluorescent signals from surface contaminants.

Confocal Microscope Setup. The apparatus used for the single-molecule detection experiments has been described in detail.[39−41] Single-molecule measurements were carried out using a confocal microscope (Zeiss Axiovert 100) in an epifluorescence geometry.

Single-Molecule Data Collection and Analysis. (a) Diffusion. For measurements on freely diffusing molecules, tens of picomolar concentrations of hairpin were dissolved in 50 mM sodium phosphate buffer, pH 7, 50 mM NaCl, and 15 μL of this solution was placed between two clean cover slips, with a Parafilm gasket as a spacer between the cover slips. The 500 μW excitation beam was focused 10 μm into a sample cell using a 100 × 1.4 NA oil-immersion objective, and a 100 μm pinhole was used to remove out-of-focus light, resulting in an effective femtoliter sample volume. Use of tens of picomolar concentrations reduced the probability of finding two molecules in the beam simultaneously to ∼0.0005. Bursts of fluorescence photons were emitted as dye-labeled hairpin molecules diffused in to and out of the excitation beam. These bursts were recorded over 5−10 min intervals, with an integration time of 1 ms, and the time traces of bursts were analyzed to collect statistics on the hairpin samples. A more detailed account of diffusion spFRET analysis has been given.[35,42] For this work, the donor and acceptor channels were examined individually, rather than summed, and the threshold for events was set at 10 times the standard deviation of the background signal.

(b) Use of Oxygen Scavengers for Diffusion Data Collection. Obtaining significant numbers of high FRET events in diffusion was initially very difficult due to the poor photophysics of the acceptor fluorophore Cy5,[43] and adequate diffusion data would have been difficult to obtain without an oxygen-scavenging system. The peak at zero energy transfer efficiency arises largely due to molecules without fluorescent Cy5. Premature photobleaching of Cy5 also contributed significantly to the histogram peak at zero energy transfer efficiency because photobleaching of the acceptor fluorophore causes an immediate termination of energy transfer. The donor peak corresponds to the zero peak in a histogram that plots the number of events versus the FRET efficiency. The large zero peak made it difficult to resolve any species with energy transfer efficiencies of 0.4 or lower (Figure 3).[35] Because the reaction with oxygen is a major contributor to photobleaching, a number of oxygen scavengers were screened in order to test their ability to extend the photobleaching lifetime of Cy5. A glucose oxidase oxygen-scavenging system similar to that used by Harada et al.[44] provided some improvement in the Cy5 photostability; however, it was not compatible with chemical or thermal denaturation experiments. We tested several small-molecule scavengers such as imidazole, β-mercaptoethanol, Trolox (a water-soluble version of vitamin E), and propyl gallate.[45] Trolox (500 μM) and propyl gallate (500 μM) were found to be very effective oxygen scavengers, and their use was found

(38) Moy, V. T.; Florin, E. L.; Gaub, H. E. *Science* **1994**, *266*, 257−259.

(39) Ha, T.; Enderle, T.; Chemla, D. S.; Weiss, S. *IEEE J. Sel. Top. Quantum Electron.* **1996**, *2*, 1115−1128.

(40) Ha, T.; Chemla, D. S.; Enderle, T.; Weiss, S. *Appl. Phys. Lett.* **1997**, *70*, 782−784.

(41) Ha, T.; Chemla, D. S.; Enderle, T.; Weiss, S. *Bioimaging* **1997**, *5*, 1−6.

(42) Dahan, M.; Deniz, A. A.; Ha, T. J.; Chemla, D. S.; Schultz, P. G.; Weiss, S. *Chem. Phys.* **1999**, *247*, 85−106.

(43) Widengren, J.; Schwille, P. *J. Phys. Chem. A* **2000**, *104*, 6416−6428.

(44) Harada, Y.; Sakurada, K.; Aoki, T.; Thomas, D. D.; Yanagida, T. *J. Mol. Biol.* **1990**, *216*, 49−68.

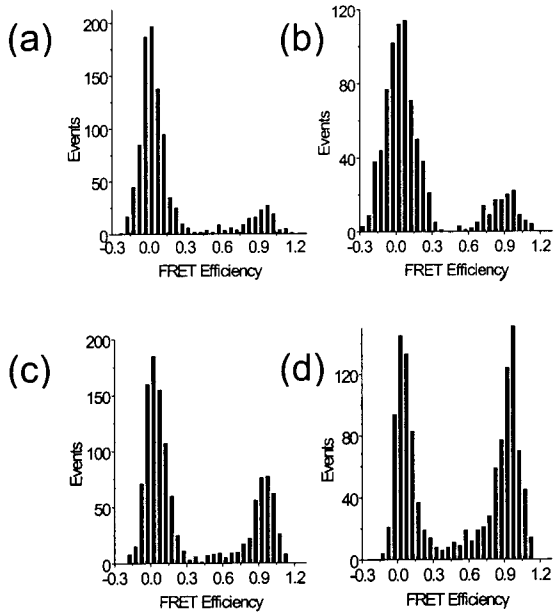

Figure 3. The use of oxygen scavengers greatly improves Cy5 fluorescence lifetimes for single hairpins in diffusion. Histograms of events versus FRET efficiency are plotted for the dA30s9 hairpin using (a) no scavenger, (b) glucose oxidase, (c) trolox, and (d) propyl gallate.

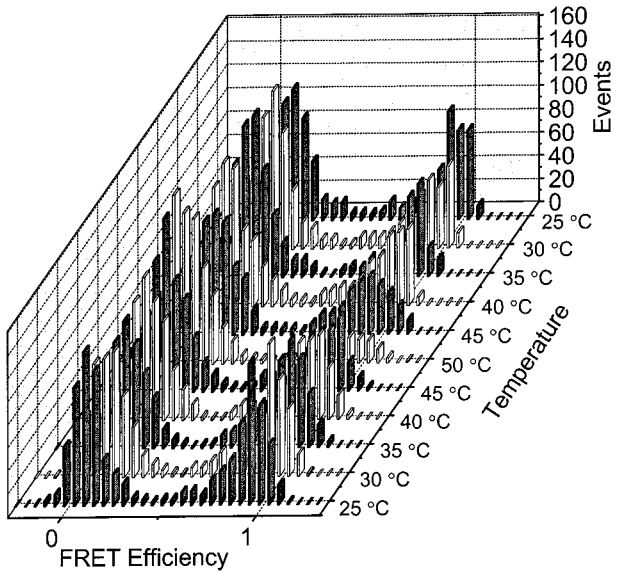

Figure 4. Temperature denaturation and renaturation of the dA40s9 hairpin in single-molecule diffusion. The FRET efficiency of fluorescence bursts from hairpins at 1 ms integration time was analyzed and plotted as a function of temperature for the same hairpin sample. Each histogram is normalized to include 1000 diffusion events.

to dramatically decrease the photobleaching and oxidative damage of Cy5 (Figure 3).

(c) Images. Images of immobilized dually labeled hairpin in a 50 mM phosphate buffer, pH 7 solution were recorded. For surface-immobilized molecules, images of dye-labeled hairpins were acquired by scanning the sample across the excitation beam. Images of 128 × 128 pixels were obtained by collecting data simultaneously per pixel on the donor and acceptor fluorescence channels with 5 ms/pixel time resolution. The image of a single molecule at 78 nm/pixel is on the order of 5 pixels in diameter, effectively imaging the diffraction-limited laser spot focused with the 1.4 NA objective. The images were then analyzed pixel by pixel via an algorithm that first subtracted the backgrounds from both images, including any donor leakage onto the acceptor channel, and then calculated the pixelwise spFRET efficiencies. Calculating the spFRET efficiencies per pixel rather than over the entire point-spread functions allowed the calculation to be done faster and also minimized the effect of photobleaching on the mean value of the transfer efficiency, but resulted in a greater contribution of shot noise to the measurement. The thresholding used for image events was identical to that used for diffusion measurements.

(d) Time Traces. Time traces, or records of the fluorescence intensities as a function of time, of immobilized single molecules were collected using a searching algorithm as previously described.[40] These time traces were analyzed individually to determine the presence of opening and closing events of the DNA hairpins. An average background signal level for each detector was calculated after fluorophore photobleaching, and this background was subtracted from each point in the corresponding fluorophore time trace. The energy transfer efficiency as a function of time was calculated from the individual time traces using eq 3. The durations of individual high-energy transfer events (closed states) and low-energy transfer events (open states) were tabulated from the respective energy transfer efficiency time traces. These tabulated durations were binned into histograms and fit to exponential decay curves. The open and closed lifetimes were calculated from the exponential fits.

(e) Polarization Anisotropy. The value obtained for FRET efficiency is dependent on the Förster radius (R_o), of the dye pair used, which is in turn dependent on the orientational factor, κ^2. R_o was calculated to be 53 Å for the tetramethylrhodamine (TMR) and cyanine-5 (Cy5) pair. This value assumes an orientational factor of 2/3 for κ^2, which must be justified by polarization anisotropy measurements of the rotational freedom of both fluorophores. We followed the method of Ha et al.[46] and measured the s and p polarization components of single donor and acceptor fluorophore emissions for the various sample preparations used in our study. These measurements were then fit with an angle parameter that provided information on the freedom of rotation of the fluorophores during the data acquisition time scale.

Results and Discussion

Diffusion Data at the Single-Molecule Level. Thermally and chemically denatured DNA hairpins were studied using single-molecule diffusion experiments (Figure 4). All hairpins showed a peak at >95% energy transfer, the relative area of which decreased with increasing temperature or denaturant concentration. Data were acquired on hairpins heated from 25 to 50 °C and cooled back to 25 °C, in 5 °C intervals. For example, as the temperature of the nine-stem hairpin was increased from 25 to 50 °C, the high-energy transfer peak decreased in area by 60.4%, with a corresponding increase in the zero energy transfer peak area of 53.5%. This behavior was reversed upon cooling of the sample from 50 to 25 °C, indicating the denaturation and reannealing of the DNA hairpins. Relative quantum yields, spectral position, and polarization anisotropy varied less than 20% between 0 and 8 M urea and between 0 and 50 °C; thus, the changes in energy transfer measured in urea and temperature denaturation experiments are due primarily to hairpin unfolding. We can deduce that the reaction time for the opening and closing of the hairpin is slower than the time of diffusion, 100−300 μs at room temperature, through the beam because the peak at high transfer efficiency decreases in amplitude for the dA40s9 hairpin as the sample is heated or urea is added (data not shown) rather than shifting to lower efficiency values. If the conformational fluctuation rates were faster than the rate of diffusion, the high FRET peak would gradually shift to lower FRET efficiency values as the sampled conformations are averaged over time.[35]

(45) Tsien, R.; Waggoner, A. In *Fluorophores for Confocal Microscopy: Photophysics and Photochemistry*; Pawley, J. B., Ed.; Plenum Press: New York, 1989; pp 169−178.

(46) Ha, T.; Glass, J.; Enderle, T.; Chemla, D. S.; Weiss, S. *Phys. Rev. Lett.* **1998**, *80*, 2093−2096.

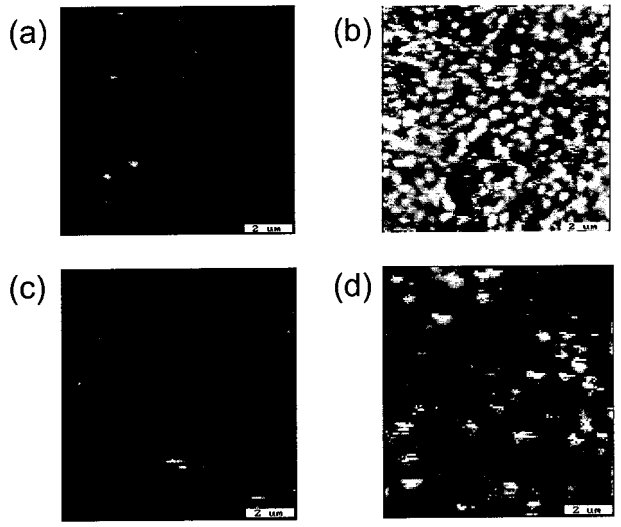

Figure 5. Surface preparation biospecificity and chemoselectivity. Non-biotinylated DNA does not bind (a), while biotinylated DNA binds epoxide-linked streptavidin-coated cover slips (b). DNA derivatized with a 3′-carboxylic acid group does not react with mercaptopropyl-silanized (MPS) glass cover slips (c), while disulfide-protected DNA undergoes a disulfide exchange reaction with the thiol-derivatized surface (d).

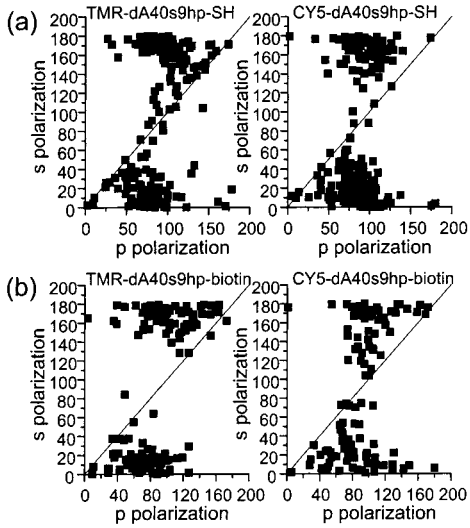

Figure 6. Polarization anisotropy data of dA40s9 hairpins bound via MPS or biotinylated BSA−streptavidin surface preparations. Data clusters around 90° and 180° indicate freely rotating fluorophores, while points that lie along the line $y = x$ indicate fixed fluorophores. Variation about 90° and 180° indicates limited fluorophore rotation. The majority of dye molecules are rotating for disulfide-linked hairpins (a) and biotin−streptavidin-linked hairpins (b).

The rate constants for the closing were predicted to be approximately 300 s^{-1} for both hairpins, while the rate constants for the opening of the hairpins were predicted to be approximately 15 and 0.3 s^{-1} for the dA40S7 and the dA40S9 hairpin, respectively.

Specificity of Surface Immobilization Chemistries. We tested the biotin−streptavidin and the disulfide bond immobilization techniques to determine whether the linkages to the glass were biospecific or chemospecific, respectively. To determine if the DNA hairpins were non-specifically bound to the surface by charge interactions, images at 50 mM and 1 M NaCl were compared. The images showed similar coverage by the hairpins, indicating minimal surface charge effects. Non-biotinylated DNA hairpins did not bind to the epoxide-linked streptavidin-coated surface (Figure 5a), while the same concentration (200 nM) of biotinylated hairpin was found to bind very well. This biospecific conjugation could be quantitated by image analysis. Images were converted to gray scale and examined using a histogram of pixel intensity. The image in Figure 5a was found to have a mean intensity of $0.39 \pm 1.77 \times 10^{-3}$ (arbitrary units), while the image in Figure 5b had a mean intensity of 80.8 ± 0.39. The errors are the standard errors of the mean, the standard deviation divided by the square root of the number of data points used in the mean calculation. Assuming a normal distribution, there is a >99% probability that the mean intensity lies within 1 unit of the value reported. A blank cover slip looks very much like the control images. Biotinylated BSA−streptavidin-coated surfaces show the same specificity as the epoxide-linked streptavidin surfaces (data not shown). Images 5a,b were obtained with DNA concentrations higher than that used to achieve single-molecule coverage in order to show conclusively that the surface preparation was biospecific. An oligonucleotide at 100 pM with a 3′-carboxylic acid group interacted minimally with the thiol-derivatized surface (Figure 5c). The image of the carboxylic acid oligonucleotide had a mean intensity of 8.99 ± 0.039, while the accompanying image of the 100 pM sulfhydryl-functionalized hairpins shown in Figure 5d had a mean intensity of 23.9 ± 0.10, indicating that the hairpin with the thiol group attaches preferentially, with a specificity of greater than 10:1 based on the number of spots, to the thiol-derivatized surface. In addition, hairpins bound to the surface via disulfide bonds could be removed from the surface with β-mercaptoethanol.

Polarization Anisotropy of Immobilized Hairpins. The DNA hairpins used in this study were designed to produce very large conformational changes that result in "on or off" energy transfer values; when the hairpin is closed, the energy transfer efficiency in all hairpins studied is high (~0.9), and when the hairpin is open, the energy transfer efficiency drops to zero. While the precise distance between the fluorophores used in our kinetics study was of secondary interest, determining the status of the rotational freedom of the fluorophores used was important in order to rule out any large changes in FRET due to rotational effects alone. In addition, the rotational properties of the dyes can provide information on the conformational freedom of the DNA hairpins themselves; e.g., if the dyes are immobilized, the hairpin is also likely to be kinetically trapped on the surface. It should be noted that what appears to be free rotation on the time scale of data acquisition does not necessarily translate to a value of 2/3 for κ^2; however, information about the average rotational freedom of the dye can be obtained. Time traces of freely rotating fluorophores show anticorrelated behavior on the p and s polarization channels, while fixed fluorophores show correlated behavior.[46] Data compiled over many single molecules is plotted as the angle parameter-fitted p angles versus the s angles (Figure 6). Freely rotating fluorophores cluster around 90° and 180° (anticorrelated), while fixed fluorophores lie along the line $y = x$ (correlated). Scatter around these two regimes indicates that there is some type of restricted rotational motion of the fluorophores. The biotin−streptavidin surface preparation appears to offer slightly better fluorophore rotational freedom than the disulfide linkage. This may be attributable to an increase in surface interactions on the neutral mercapto-silanized glass surface over those on the negatively charged surface of the biotin−streptavidin surface preparation, which underwent additional quenching of the epoxy-silane-derivatized surface by aspartic acid. In both cases, however, the majority of the fluorophores show significant

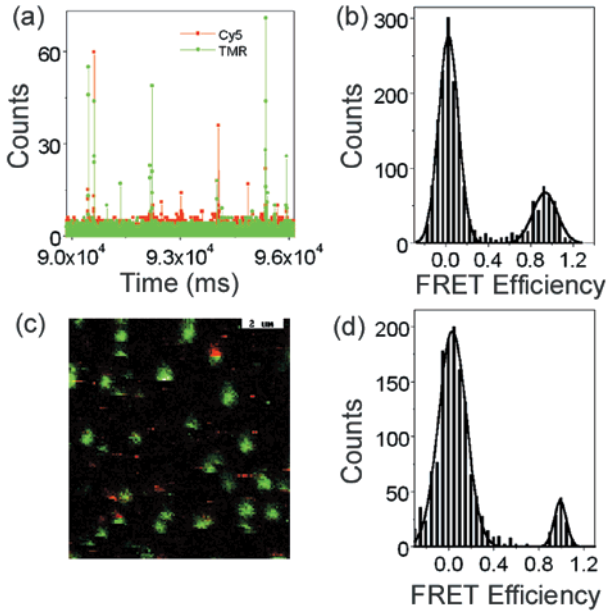

Figure 7. Example of diffusion (a) and image (c) data and analyses. Donor emission is shown in green and acceptor emission in red. The image is an overlay of simultaneously acquired donor and acceptor images. Histograms are fit with Gaussian distributions. The high FRET peak position shows greater than 90% energy transfer efficiency for both diffusing (b) and immobilized hairpins (d). The width of the Gaussian fit to the zero peak is slightly larger for the image data than for the diffusion data, due to the higher acceptor background for surface-immobilized hairpins. The image is formed by scanning from left to right, top to bottom. Evidence that we are observing single-pair FRET can be found in image (c) in which the abrupt disappearance of the acceptor fluorescence (shown in red) upon acceptor photobleaching is accompanied by the emergence of the donor fluorescence (shown in green).

degrees of rotational freedom, consistent with low interaction of the fluorophores with the glass surface.

Comparison of Diffusion and Immobilized Hairpins. Energy transfer efficiency histograms of DNA hairpins immobilized through a disulfide bond to the glass cover slips and freely diffusing in solution are compared in Figure 7. Evidence that we are observing single-pair FRET can be found in image 7c in which the abrupt disappearance of the acceptor fluorescence (shown in red) upon acceptor photobleaching is accompanied by the emergence of the donor fluorescence (shown in green). Data for the biotinylated hairpins and streptavidin-coated cover slips look similar to those shown for the disulfide-derivatized hairpins. Diffusion data were acquired at 1 ms time resolution, and the results indicated that fluctuations occurred on a time scale slower than 100−300 μs, the time of diffusion through the excitation beam. The closed-state lifetimes of the hairpins are also greater than the 5 ms/pixel image time resolution, consistent with calculated closed-state lifetime values of 70 ms and 3.8 s for the dA40S7 and dA40S9 hairpins calculated from published FCS and thermodynamic data. The calculated open-state lifetime of 3 ms is too close to the time resolution to measure in an image. Energy transfer efficiency histograms from image and diffusion acquired data were fitted with Gaussian distributions. The width of the peak at zero energy transfer efficiency for the surface measurement is significantly broader than the peak in diffusion (0.25 versus 0.19) due to the increased acceptor channel background that accompanies surface data. The comparable distributions of FRET events for image and diffusion data, along with the polarization data, indicate that while in some cases there is evidence of interaction between either the fluorophores or the DNA and the derivatized surface, the overall behavior of the immobilized DNA hairpins is similar to that of hairpins in diffusion.

The Effect of Stem Size on Opening and Closing Rates of DNA Hairpins. We monitored individual surface-immobilized dA30S14, dA40S7, and dA40S9 hairpins as a function of time to study the dynamics of the DNA fluctuations. Here, the streptavidin−biotinylated BSA surfaces were used for immobilization because of their attachment specificity. Searches for molecules were accomplished by looking for emission from both donor and acceptor fluorophores. While the majority of molecules showed high degrees of energy transfer, no individual opening and closing events were observed out of over 1000 dA30s14 hairpin molecules sampled using the disulfide immobilization method. The lack of measured opening and closing events for the 14-stem hairpin was due primarily to the limitations of the fluorescence technique used. Since the opening and closing rates for this hairpin were quite long, photobleaching of the fluorophores became a significant problem in the data acquisition. Many of the dA40S7 and dA40S9 hairpins also showed constant FRET efficiency until fluorophore photobleaching regardless of integration times that ranged from 0.2 to 25 ms. Opening and closing events were observed in 5 out of 200 (2.5%) of the dA40s7 hairpin time traces and in 34 out of 1000 (3.4%) of the dA40s9 hairpin time traces. Statistics on the conformational fluctuations were collected with these hairpins using the streptavidin−biotinylated BSA surface. It was proposed that the hairpins were interacting with the surface and therefore inhibiting the observation of conformational fluctuations of the hairpins. A dA40S9 hairpin with a longer ethylene glycol linker between the DNA and the surface-attaching group did not demonstrate more folding events for the dA40s9-thiol hairpin.

The photophysical behaviors of the fluorophores were taken into account when determining whether an observed time trace contained an opening or closing event. The addition of oxygen scavengers had the undesirable effect of lengthening the triplet-state lifetimes of fluorescent dyes, since molecular oxygen acts as a triplet-state quencher; therefore, oxygen scavengers were used only in diffusion measurements. In addition, fluorescent dyes are known to have long dark states in which fluorescence is quenched. Both of these effects were considered when deciding whether an anticorrelated change in donor and acceptor emission intensities was, in fact, an opening or closing event. Figure 8 shows time traces taken on dA40s7 and A40s9 hairpins at a 10 ms integration time. The fluorescence signal in the TMR (red) channel in the Figure 8a time trace is higher than that in the 8b time trace due to higher backgrounds that are attributed to variability in cover slips used. The advantage of using single-pair FRET rather than the single fluorophore quenching of molecular beacons for fluctuation measurements is evident in the time traces; it is easy to determine which fluctuations are due to conformations of the DNA and which are due to the photophysical behaviors of the dyes. For example, the open states of the hairpins shown in Figure 8a,b differ from dark states of the acceptor because the acceptor fluorescence does not return to the background level but remains at $E = 0.2$. Leakage of donor fluorescence onto the acceptor channel would result in a false positive FRET efficiency signal of approximately 0.1, while for dark states of the donor, only a low signal due to direct excitation of the acceptor fluorophore would be observed. The relatively long integration time used for time traces (at least 5 ms/point) effectively removes the complication of triplet states (typically of the order of microseconds) in the measurements.

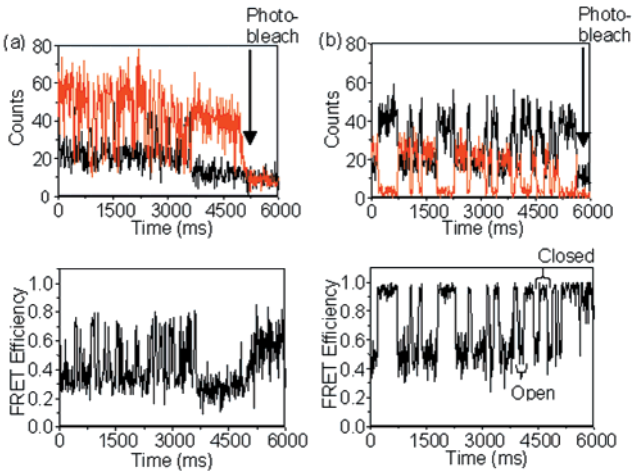

Figure 8. Examples of TMR and Cy5 fluctuations as functions of time at a data acquisition rate of 10 ms for biotin−BSA−streptavidin-immobilized hairpins (a) dA40s7 and (b) dA40s9. The top graphs show the Cy5 (acceptor) fluorescence in black and the TMR (donor) fluorescence in red. The bottom graphs are the calculated energy transfer efficiencies (eq 3) for the corresponding time traces shown above. High Cy5 (black) and low TMR (red) signals indicate a closed hairpin, while low Cy5 (black) and high TMR (red) signals indicate an open hairpin. An energy transfer signal of 0.5 or less was considered to be an open hairpin. The time traces shown (top) are representative samples of time trace data and their conversion into the plots of FRET efficiency as a function of time (bottom) using eq 3. The time traces for the dA40S7 and dA40S9 hairpins look different because the dA40S7 hairpin spends less time in the closed state than the dA40S9 hairpin. In addition, the TMR background signal (red) is higher for the dA40S7 hairpin in (a) than for the dA40S9 hairpin in (b) due to the variability in the batch of cover slips used. The times that a hairpin showed a high FRET event (closed-state lifetime) and a low FRET event (open-state lifetime) were measured by hand and compiled into histograms as depicted in Figure 9.

The time that the hairpin is open or closed was measured as the duration of an observed low- or high-energy transfer event, respectively. The durations of 39 high FRET events and 39 low FRET events were measured for the dA40s7 hairpin, and 98 high FRET and 94 low FRET events for the dA40s9 hairpin. For a simple reversible two-state process, such as that shown in Figure 1, exponential distributions for the closed- and open-state lifetimes are expected due to the Poisson nature of the process.[47] Deviations from single exponentials would be indicative of a more complex kinetic process, such as genuine intermediates or immobilization artifacts such as kinetic trapping of the dyes or DNA on the surface. Single-exponential fits to the distributions are shown in Figure 9; more complex functions are not warranted given the limited size of the data sets.

We observed exponential kinetics for the opening times of both the dA40S7 and dA40S9 hairpins that scaled consistently with their stem size. The dA40s7 hairpin was found to have a closed time of 45 ± 2.4 ms, while the dA40s9 hairpin had a closed time of 103 ± 6.0 ms. The seven-stem hairpin had an open time of 133 ± 5.5 ms, and the nine-stem hairpin had an open time of 142 ± 22 ms. Exponential fits to the data were performed using a Chi^2 test and reflect a 95% confidence level in the fits to the data. Using the exponential fits to the rate data shown in Figure 9, we calculated the equilibrium constant for closing, $K_{closing}$, of the dA40S7 and dA40S9 hairpins (eq 1). Using the respective $K_{closing}$ values, the Gibb's free energy for the closing of both hairpins at 298 K was calculated (eq 2).

(47) Colquhoun, D.; Hawkes, A. G. *Single-Channel Recording*, 2nd ed.; Plenum: New York, 1995.

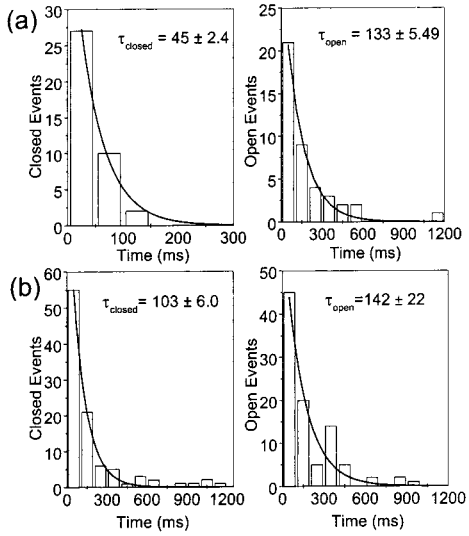

Figure 9. Exponential fits to closed and open time (high and low FRET signals) for (a) dA40s7 and (b) dA40s9 hairpins. Fits assume two-state folding kinetics. Close-time bin width for the dA40s7 hairpin is 50 ms, while open-time bin width is 100 ms. Closed-time bin width for the dA40s9 hairpin is 100 ms, and open-time bin width is also 100 ms.

The experimentally derived $\Delta G_{closing}$ values for the dA40S7 and dA40S9 hairpins were 0.65 ± 0.05 and 0.19 ± 0.11 kcal/mol, respectively. The closed dA40S9 hairpin was determined to be approximately 0.45 ± 0.15 kcal/mol more stable than the closed dA40S7 hairpin. These results show that the immobilized hairpins spend more time in an open state than in a closed state; thus, the open state is stabilized with respect to the closed state.

A single set of parameters has been derived from 108 oligonucleotide duplexes from six different studies to give a unified view of polymer, dumbbell, and oligonucleotide DNA nearest-neighbor thermodynamics that accounts for experimental temperature and that corrects for differences in salt concentration.[27,28] The calculated $\Delta G_{closing}$ values, predicted by the unified view of oligonucleotide stability from SantaLucia, were −1.8 ± 0.09 and −4.2 ± 0.21 kcal/mol for the dA40S7 and dA40S9 hairpins, respectively. The experimentally derived $\Delta\Delta G_{closing}$ value of 0.45 ± 0.15 kcal/mol is 5.3 times lower than the nearest-neighbor calculations of hairpin stability in solution in equivalent NaCl concentrations at 25 °C. The measured open-state lifetime is about 30 times longer than the approximated calculated open-state lifetime of 3 ms for both hairpins based on extrapolation from a previous study. The measured closed-state lifetimes are 1.5 times shorter for the dA40S7 hairpin and 40 times shorter for the dA40S9 hairpin. The longer-than-expected open-state lifetime may be due to an increase in open-state stability due to interactions with the derivatized glass surface; however, Bonnet's hairpin, studied by FCS in diffusion, with five base pairs in the stem and 21 adenosines in the loop, also favored the open state over the closed state by a slight margin ($\Delta G_{closing} \approx 0.13$ kcal/mol). Nearest-neighbor theory, however, predicts this 21 adenosine-loop hairpin to be closed with a $\Delta G_{closing}$ value of −1.8 ± 0.09 kcal/mol. Using this value, and the experimental open-state lifetime from the work of Bonnet et al., we approximate the closed-state lifetime to be 12 ms, a value that is 30 times longer than the experimental value of 0.4 ms. This predicted closed-state lifetime for the adenosine-loop hairpin reported by Bonnet et al. is larger than the experimental value by the same magnitude as the dA40S9 calculated and experimental results described in this study. In contrast with the adenosine-loop hairpins from the study reported

by Bonnet et al., the thymidine-loop hairpins from the same study (stem is identical) have experimental closed-state lifetimes that are in reasonable agreement with the values calculated using nearest-neighbor theory to predict the Gibb's free energy of the system. These results are supported by a recent study by Goddard et al., where it was determined that hairpins with a poly(A)-loop sequence had an enthalpic rigidity consistent with base stacking, whereas hairpins with a poly(T)-loop sequence displayed a purely entropic elasticity, consistent with the notion that ssDNA acts as a random coil.[48] Furthermore, this study showed that the closed-state lifetime of poly(A)-loop hairpins was independent of loop length or sequence, implying that the closed loop is a random coil with no influence on stem stability. These findings showed that the open-state lifetime increases as the loop size increases for poly(A)-loop hairpins, and they directly show that the scaling model derived for poly(T) hairpins is inadequate for describing poly(A)-loop hairpins. The increased open-state lifetime that we found for our A40 hairpins is consistent with the experiments of Goddard et al. and is inconsistent with the explanation that the open state of the hairpin is longer than predicted solely due to interaction with the derivatized glass surface. Our experiments show that specificity of binding, however, is not a guarantee that significant effects on the rates and stabilities of the biomolecule being studied will not be observed. The disagreement between our experimentally measured $\Delta\Delta G_{\text{closing}}$ value and the calculated value and our longer open-state lifetimes and shorter closed-state lifetimes is significant, and it implies that in the simple use of a scaling factor to determine open-state lifetimes on the basis of previous work on shorter thymidine-loop hairpins and in the use of nearest-neighbor theory to predict closed-state lifetimes, the effects of sequence-dependent rigidity on the single-stranded phase must be considered in order to accurately predict the folding dynamics of ssDNA.

Conclusions

spFRET was used to measure the denatured and folded-state lifetimes of DNA hairpins at single-molecule resolution. We have shown that oxygen-scavenging systems can greatly enhance fluorophore characteristics so that single-molecule diffusion data can be obtained. We have described three different surface immobilization techniques that are suitable for obtaining data at single-molecule resolution, and we describe diffusion and surface immobilization techniques that will be useful in the characterization of biomolecules at the single-molecule level.

The open- and closed-state lifetimes of surface-immobilized hairpins follow the kinetics obtained from diffusion measurements, and the two-state kinetics of the system are preserved. The longer open-state lifetimes and the shorter closed-state lifetimes of the hairpins indicate that tethering the hairpins to a surface appears to stabilize the open state of the hairpin and thus affects the overall kinetics of the system. Nearest-neighbor theory poorly predicts the stability of a five-base-pair stem hairpin with 21 adenosines in its loop while accurately predicting the stability of an identically stemmed hairpin with either 21 of 30 thymidines in their loops. Therefore, application of the scaling model derived from polymer simulations and the thermodynamic calculations based on nearest-neighbor theory also may not be as simple for larger hairpins with many adenosines in their loops.[19,27,28,48−51] Although a study of shorter hairpins might have been instructive, we were limited to studying longer hairpins because the fluctuations of shorter hairpins used in previous diffusion were too fast for the fastest data acquisition rate (200 μs) of these single-molecule experiments.[19,35]

We show that single-molecule experiments allow direct measurement of the kinetic properties of biological systems, observations of events that are difficult if not impossible to detect at the ensemble level in the absence of synchronization, and examination of the distribution of properties within a population. The sensitive distance dependence of FRET measurements along with the surface immobilization and time trace analysis techniques described in this study may allow experimentation on more complex hairpin kinetics. For example, single-molecule FRET experiments may prove useful in studying the poorly understood kinetics of multiple alternate hairpin structures due to triplet base repeats (sliding hairpins) at sites of gene transcription and translation regulation that are thought to result in genetic diseases such as fragile X syndrome and myotonic dystrophia.

Acknowledgment. Financial support for this work was provided by the National Institutes of Health (Grant No. GM49220) and by the National Science Foundation under Grant No. CHE-971-4390. We thank T. Laurence for his valuable help in programming and data analysis. J.R.G. thanks Prof. Carolyn Bertozzi for her support during the completion of this work. J.L.G. acknowledges the generous support of the National Physical Sciences Consortium and Lawrence Livermore National Laboratory. P.G.S. was a Howard Hughes Medical Investigator during the course of this work. J.R.G. and J.L.G. contributed equally to this work.

JA0027620

(48) Goddard, N. L.; Bonnet, G.; Krichevsky, O.; Libchaber, A. *Phys. Rev. Lett.* **2000**, *85*, 2400−2403.

(49) Podtelezhnikov, A.; Vologodskii, A. *Macromolecules* **1997**, *30*, 6668−6673.

(50) Wilemsky, G.; Fixman, M. *J. Chem. Phys.* **1974**, *60*, 866−877.

(51) Berg, O. *Biopolymers* **1984**, *23*, 1869−1889.